Molecular Thermodynamics for Swelling of a Mesoscopic Ionomer Gel in 1:1 Salt Solutions

A Victorov[1], C Radke[2], and J Prausnitz[2,3]

1. *Department of Chemistry, St.Petersburg University, 198504 St.Petersburg, Russia; e-mail: alexi@nonel.pu.ru*
2. *Department of Chemical Engineering, University of California, Berkeley, CA 94720-1462;*
3. *Chemical Sciences Division, Lawrence Berkeley National Laboratory, Berkeley, CA 94720, USA*

Abstract

For a microphase-separated diblock copolymer ionic gel swollen in salt solution, a molecular-thermodynamic model is based on the self-consistent field theory in the limit of strongly segregated copolymer subchains. The geometry of microdomains is described using the Milner generic wedge construction neglecting the packing frustration. Thermodynamic functions are expressed analytically for gels of lamellar, bicontinuous, cylindrical and spherical morphologies. Molecules are characterized by chain composition, length, rigidity, degree of ionization, and by effective polymer-polymer and polymer-solvent interaction parameters.

The model predicts equilibrium solvent uptakes and the equilibrium microdomain spacing for gels swollen in salt solutions. Results are given for details of the gel structure: distribution of mobile ions and polymer segments, and the electric potential across microdomains. Apart from effects obtained by coupling classical Flory-Rehner theory with Donnan equilibria, viz., increased swelling with polyelectrolyte charge and shrinking of gel upon addition of salt, the model predicts the effects of microphase morphology on swelling.

Introduction

Because polymer gels show a variety of structure-property relations, they find numerous applications in the design of biomedical materials [1], drug-release systems [2], cosmetics, food technology and other rapidly developing areas. Especially important are ionic gels whose swelling and elastic properties depend on electrostatic interactions that are sensitive to pH and salinity.

The effect of aqueous salt on swelling of ionic gels has been studied experimentally and theoretically. Most authors consider chemically-crosslinked polymethacrylate- [3-13] or polyvinylpyridine-based [14] gels. Ionic gels can swell more than neutral gels; the extent of swelling depends on the degree of ionization and on the ionic strength of the external solution. An increase of ionic strength leads to abrupt deswelling of swollen ionic gels such that the extent of swelling becomes similar to that of a nonionic gel. Depending on chemical composition and ionic charge of the gel, this deswelling may be observed at different salinities ranging from ca. 1 to ca. 100 mM [3-14]. At sufficiently large ionic strength, swelling is no longer sensitive to the polymer's degree of ionization or to ionic strength. Further addition of salt to the external solution leads again to noticeable swelling of an ionic gel [6, 10]. Swelling behavior is not sensitive to the nature of added monovalent cations [3, 13]. Divalent [7, 13] and trivalent [11] cations have a stronger effect on swelling of a gel than the monovalent cations. An important factor is the nature of a multivalent ion [11]. For weak polyelectrolyte gels, the ionization degree may depend substantially on pH and salinity of the surrounding solution. This effect, called charge regulation, may result in another region of gel deswelling at low salt concentration, e.g., at 0.01 - 0.1mM for gels considered in refs.[10, 14].

One of the key factors controlling the properties of a gel is its heterogeneous composition. Formation of nanodroplets and bicontinuous structures inside the gel may substantially affect its thermodynamic properties and phase behavior. Interest in gels having a well-developed

mesostructure and morphology has been growing within the last several years because morphological changes in response to variation of external conditions may provide a basis for developing new types of environmentally sensitive, intelligent materials. Extensive experimental work has been directed at producing new block-copolymer materials that are capable of assembling into a variety of mesostructures. Fascinating structures of ionic block-copolymer self-assembling systems (physical gels in particular) have been described in the work of Eisenberg and his school [15-17]. Block copolymers that are built by combining hydrophobic subchains and hydrophilic ionic subchains [18] may form a rich variety of mesostructures including vesicles, crew-cut or starlike micelles and gels of different morphology [19-22]. These systems are often stimulus-responsive. Formation of a specific structure depends on the relative length of the ionic and nonionic parts of the molecules, solvent composition, temperature, salt content and pH. An example of a mesostructure gel of particular relevance to biomedical applications such as contact lenses is a physical co-continuous oxyphilic-hydrophilic-lipophilic block-copolymer gel [23] that allows simultaneous permeation of water, oxygen and heptane via three cocontinuous channels.

The classical theory of Flory and Rehner [24], combined with that of Donnan, reflects the basic trends in swelling behavior of an ionic gel in 1:1-salt solutions. Ideal Donnan osmotic equilibria account for the deswelling of an ionic gel upon addition of salt [6, 7, 10-14]. When the gel's degree of ionization depends on the concentration of salt, introducing the gel ionization-equilibrium constant accounts for deswelling of the gel at low salt concentration due to charge regulation [10, 14]. However, this simple theory does not explain an upturn of swelling in the limit of high ionic strength [10].

Classical theory describes the polymer gel in terms of average characteristics and does not reflect the gel's structural inhomogeneity and morphology. However, considerable progress has been made in understanding the structure and properties of polyelectrolyte brushes [25] in salt solutions [26-30]. Both annealed (with charge regulation) [27, 28] and quenched (carrying a fixed

charge) [29, 30] polyelectrolyte brushes immersed in salt solution have been considered using self-consistent field theory [27, 31]. The nonmonotonic dependence of average brush thickness on ionic strength [27, 28, 32] is similar to the nonmonotonic effect of salt on gel swelling. Different regimes controlling swelling and elastic behavior of polyelectrolyte brushes have been described using scaling relations [25, 33]. The success in describing polymer brushes suggests a similar approach for polyelectrolyte mesostructured systems.

Spherical and cylindrical ionic block copolymer micelles and bilayers have been modeled by Zhulina and Borisov [34], who combined the self-consistent field theory for a strongly stretched polymer brush with the Poisson-Boltzmann equation and with the local-electroneutrality assumption to model electrostatics. Two recent models of polyelectrolyte gels reflect characteristic features of the mesocsopic structure: the so called swiss-cheese structure of an ionic gel swollen in salt solution [35], and a sequence of self-assembling structures in a solution containing an associating, strongly segregated polyelectrolyte [36].

In our previous publications [37, 38] we considered nonionic gels of different morphology swelling in a salt-free solvent. We proposed an analytical model based on self-consistent field theory in the strong-segregation limit. In this work we continue along the same line and discuss the properties of mesoscopic ionic gels (ionic gels having lamellar, bicontinuous, cylindrical or spherical domains) swollen in brine. The prototype for the system considered here is a copolymer gel used, for example, for fabricating extended-wear contact lenses: segregated silicone and hydrogel microphases may form nanodroplets and bicontinuous structures. Hydrophilic parts of the polymer chains that swell in tears are capable of immobilizing some charge at specific functional groups, e.g., positive charges bound to aminogroups. In this work we describe the effect of gel structure on the swelling behavior of an ionic gel. Electrostatic effects are taken into account by combining the self-consistent field theory for a swollen polyelectrolyte brush with the linearized Poisson-Boltzmann equation for polymer-free zones. The spatial distribution of

polymer segments and mobile ions and the free energy of the gel are expressed analytically in terms of the size of the microdomains inside the swollen gel. The microdomain size and equilibrium swelling are determined for different morphologies. We examine the effects of gel charge and ionic strength on equilibrium swelling. Our model is applied at conditions far beyond the range of ionic charges and salinities typical of physiological systems; we consider a weakly charged gel as well as a strongly charged gel in a solvent at low or high salt concentration.

The Model

We consider a diblock copolymer forming a swollen gel. The blocks are strongly segregated into the outer (B) and the inner (A) domains that may have lamellar, bicontinuous, cylindric, or shperical geometry (Fig.1). B-blocks are hydrophobic; swelling is due to the hydrophilic A-blocks only. Each A-chain consists of N_A segments and each B-chain consists of N_B segments. Some 1:1-salt is present in the A-domain and a known number of cations, αN_A, is immobilized by binding to each A-chain[29, 31, 39]. The fractional charge α is called the degree of ionization. Our model applies without change to the case where ionization of A-chains is caused by dissociation of ionic groups of the polymer. Assuming strongly stretched polymer chains, the Helmholtz energy of the gel (F^{gel}) includes independent surface, mixing and chain-stretching contributions. The effective self-consistent field acting on polymer segments is parabolic in the distance from the A-B interface [29, 30], regardless of the type of intermolecular interactions in the system. In the free energy of mixing, the nonelectrostatic contribution (F^{mix}_{nonel}) is considered separately from the electrostatic part (F^{ion}) of the gel free energy. Thus [25, 31, 37, 38]:

$$F^{gel} = \sigma_{AB}\boldsymbol{A} + F^{str}_{A} + F^{str}_{B} + F^{mix}_{nonel} + F^{ion} \tag{1}$$

where σ_{AB} is the bare interfacial tension (i.e., the tension of a flat A–B interface unperturbed by curvature effects or by presence of solvent) and $\boldsymbol{A}$ is the surface area of a sharp interface between

A- and B- domains; the stretching terms for A- and B-subchains, F_A^{str} and F_B^{str}, are expressed as $F_p^{str} = B_p \int x^2 c_p dV$, where $B_p = \frac{3\pi^2}{8N_p^2 a_K^2}$ is the elasticity constant of a subchain p (p=A,B); a_K is the Kuhn segment length, x is the distance from the interface, c_p is the local polymer concentration, and the integration is over the gel volume; here and below the energies are given in k_BT-units. The interfacial tension is estimated as $\sigma_{AB} = (\chi_{AB}/6)^{1/2} / a_K^2$, where χ_{AB} is the Flory interaction parameter for segments A and B [40, 41].

Analytical results can be obtained [29, 31] when we assume that the ions are point-charges and a dilute-gas expression for the local entropy terms:

$$F^{ion} = W^{el} - TS^{el} = \int \rho_+ (\ln \rho_+ - 1) dV + \int \rho_- (\ln \rho_- - 1) dV + \frac{1}{2} \int \Psi \rho dV \qquad (2)$$

where ρ_+ and ρ_- are the local concentrations of mobile charges; $\rho = \alpha c_p + \rho_+ - \rho_-$ is the local charge density, and $\Psi = e\psi/(k_B T)$ is the reduced electric potential ψ; e is the electron charge. The de Broglie thermal wavelength of the ions is immaterial in our derivation and therefore omitted from the logarithmic terms. Minimization of the free energy with respect to the spatial distribution of mobile charges and polymer segments gives the Boltzmann distribution of the mobile charges and an additional Euler-Lagrange equation that couples segment interactions to the elastic response of the chain [31]:

$$\alpha \Psi_I + \delta F_{nonel}^{mix} \big/ \delta c_p = const - B_A x^2 \qquad (3)$$

where Ψ_I is the reduced electric potential inside the A-chain polymer brush; the elasticity constant of the A-chain, B_A, has been defined after Equation (1). The functional derivative $\delta F_{nonel}^{mix} \big/ \delta c_p$ has the same units as F_{nonel}^{mix}, and hence all terms of Equation (3) are in reduced units. Equation (3) has no ionic valence because we consider univalent electrolytes. However all

equations of this work can be easily generalized for *z:z* symmetric electrolytes. We assume that the nonelectrostatic part of the free energy is far less sensitive to the details of segment distribution and that the structure of the gel is primarily governed by the electrostatic interactions. Thus, we assume that $\delta F_{nonel}^{mix} / \delta c_p \approx 0$. We then obtain a parabolic form of the electric potential within the polymer brush [29-31, 42]. This result implies a linear electric field inside the brush and some accumulated charge that must be compensated by a charge cloud in the solvent pool.

Gel Geometry To take into account the geometry of the gel microdomains, we apply the Milner generic wedge construction [43, 44] neglecting the "packing frustration" [45]. This method introduces one reduced spatial variable, *y*, to characterize the domain of a given geometry. In reduced units, the surface area and the volume at distance *y* from the origin are:

$$a(y) \equiv \frac{A(y)}{A(R)} = y^{\nu} \tag{4}$$

$$\mathrm{v}(y) \equiv \frac{V(y)}{RA(R)} = \frac{1}{\nu+1} y^{\nu+1} \tag{5}$$

where *R* is the size of one structural unit of the gel (Fig.1); ***A(y)*** is the surface area, *V(y)* is the volume; and ν=0, ½ , 1, 2 for lamellar, bicontinuous, cylindric and spherical morphology, respectively. Unlike our previous work [37], Equation (4) gives a different expression for ν=½ that only approximates the surface area of the Gaussian saddle in our simple model of a bicontinuous structure. The surface areas given by Equation (4) for ν= ½ are in fair agreement with those obtained from the original expression for the surface area of a Gaussian saddle [44]. The advantage of Equation (4) is that instead of the original expression, it provides a simpler form of the Poisson-Boltzmann equation.

Electrostatic Potential in the Gels of Different Morphologies The Boltzmann distribution for mobile charges can be obtained by variational minimization of the free energy given by

Equations (1) and (2) [31]. For univalent ions considered in this work, in the A-brush (zone I) and in the solvent pool inside the gel (zone II) we have:

$$\textit{zone I:} \qquad \ln\rho_+ + \Psi_I = \lambda_+ \qquad \ln\rho_- - \Psi_I = \lambda_- \tag{6}$$

$$\textit{zone II:} \qquad \ln\rho_+ + \Psi_{II} = \lambda_+ \qquad \ln\rho_- - \Psi_{II} = \lambda_- \tag{7}$$

where the Lagrange multipliers λ_+ and λ_- do not change from zone to zone because the pool and the brush are in equilibrium. In a closed system, these multipliers are determined from the condition of conservation of particles; if the gel is in equilibrium with the outside salt solution of concentration c_s^b, then $\lambda_+ = \lambda_- = \ln c_s^b$.

The electric potential in the polymer brush is found from Equation (3):

$$\Psi_I(y) = \Psi_I(\beta) - K(\beta - y)^2 \tag{8}$$

where $\Psi_I(\beta)$ is the reduced potential at the A-B interface ($y = \beta$) and $K \equiv R^2 B_A / \alpha$. The potential for the solvent pool is determined from the Poisson-Boltzmann equation:

$$\nabla^2 \Psi_{II} = -4\pi l_B \left[\rho_+^0 e^{-\Psi_{II}} - \rho_-^0 e^{\Psi_{II}}\right] \tag{9}$$

where $\Psi_{II} = e\psi_{II} / k_B T$ is the reduced potential for the solvent pool; $l_B = e^2/(k_B T \varepsilon)$ is the Bierrum length; ρ_+^0 and ρ_-^0 are local number densities of positive and negative ions at zero electric potential; hence $\ln\rho_+^0 = \lambda_+$ and $\ln\rho_-^0 = \lambda_-$. Two boundary conditions are given, respectively, by the requirement of vanishing field at the center of the pool and by the Gauss law at the polymer-solvent pool boundary:

$$\left(\frac{\partial \Psi_I}{\partial y}\right)_{y=0} = 0 \tag{10}$$

$$\varepsilon_{II}\left(\frac{\partial \Psi_{II}}{\partial y}\right)_{y=\gamma} = \varepsilon_I\left(\frac{\partial \Psi_I}{\partial y}\right)_{y=\gamma} = \frac{RQ(\gamma)}{a(\gamma)A(R)} = R\Sigma(\gamma) \tag{11}$$

where $Q(\gamma)$ is the total charge accumulated inside the polymer brush; $\Sigma(\gamma)$ is the surface charge density; ε_{II} and ε_{I} are the dielectric constants of the pool and of the swollen A-brush, respectively. Assuming that the dielectric constant does not change appreciably at the boundary between the solvent pool and the hydrophilic swollen brush, we write Equation (11) in the form:

$$\left(\frac{\partial \Psi_{II}}{\partial y}\right)_{y=\gamma} = \left(\frac{\partial \Psi_{I}}{\partial y}\right)_{y=\gamma} = \frac{2Rh}{H_0} \tag{12}$$

where $h = R(\beta - \gamma)/H_0$ is the reduced thickness of the A-brush, and $H_0 = (\alpha/B_A)^{1/2}$ is a characteristic length determined by the brush elasticity and fixed charge [29].

We now write the Laplacian as:

$$\nabla^2 \equiv \frac{1}{R^2 a(y)} \frac{\partial}{\partial y}\left[a(y)\frac{\partial}{\partial y}\right] = \frac{1}{R^2}\left[\frac{\partial^2}{\partial y^2} + \frac{\partial \ln a(y)}{\partial y}\frac{\partial}{\partial y}\right] \tag{13}$$

which is an exact expression for lamellae, cylinders, and spheres, and an approximation for the bicontinuous morphology. With this Laplacian, we use a linearized version of the Poisson-Boltzmann equation giving $\Psi_{II}(y)$ for all these geometries in terms of modified Bessel functions (see Appendix 1). The use of the linearized version of the Poisson-Boltzmann equation imposes a limitation on the model's range of applicability: low electric potentials in the solvent pool. However, the potential may be substantial in the swollen polyelectrolyte brush where we use the non-linearized Poisson-Boltzmann equation.

The potential drop within the swollen brush depends on a number of factors such as degree of chain ionization, its elasticity, length, the uptake of solvent and the salt content of the gel. Rigorous analysis of the validity of the linear Poisson-Boltzmann equation for the pool is a nontrivial issue and deserves a separate study. Strictly speaking, the linearized model is not valid in the limit of vanishing external salt. In this work we check the validity of the linear

approximation by calculating the values of electric potential at the solvent pool – polymer brush boundary. Our calculations show that even at low external solution salinities of 0.1-1mM, screening of electrostatic interactions within the brush is often sufficient to result in low electric potentials in the pool, suggesting that our approach is reliable.

Gel Free Energy The equilibrium thermodynamic potential of the gel is found by substituting the equilibrium profiles and potentials into Equations (1,2). After some algebra we obtain:

$$\frac{F^{ion}+F_A^{str}}{RA(R)}=(\lambda_+-1)\int_0^\beta \rho_+(y)a(y)dy+(\lambda_--1)\int_0^\beta \rho_-(y)a(y)dy+$$

$$+\Psi_I(\beta)\int_\gamma^\beta \alpha c_p(y)a(y)dy-\frac{W^{el}}{RA(R)} \qquad (14)$$

where the first two integrals give the total amount of positive and negative mobile charge in the brush. Applying Green's theorem to calculate the electrostatic energy, W^{el}, we see that the surface integrals vanish, leading to:

$$\frac{W^{el}}{RA(R)}=\frac{1}{8\pi l_B}\int_\gamma^\beta (\nabla\Psi_I)^2 a(y)dy+\frac{1}{8\pi l_B}\int_0^\gamma (\nabla\Psi_{II})^2 a(y)dy. \qquad (15)$$

Both integrals can be solved analytically. Upon performing some lengthy algebra we obtain:

$$\frac{W^{el}}{RA(R)}=\frac{1}{2\pi l_B H_0^2}\left\{\frac{h^2}{2}\gamma^{\nu+1}\left[1-\frac{I_{z-1}(R\kappa\gamma)I_{z+1}(R\kappa\gamma)}{I_z^2(R\kappa\gamma)}\right]+\frac{R^2}{H_0^2}I_A(\beta,\gamma)\right\} \qquad (16)$$

where $I_z(R\kappa y)$ is the modified Bessel function of order z where $z=(\nu+1)/2$, $\kappa^2=4\pi l_B\left[\rho_+^0+\rho_-^0\right]$ is the Debye screening parameter, and $I_A(\beta,\gamma)$ is the integral from the Hookian elasticity of the polymer chain [37, 38]:

$$I_A(\beta,\gamma)=\int_\gamma^\beta (\beta-y)^2 a(y)dy=$$

$$= \frac{2\beta^{\nu+3}}{(\nu+1)(\nu+2)(\nu+3)} - \gamma^{\nu+1}\left[\frac{\gamma^2}{(\nu+3)} - \frac{2\beta\gamma}{(\nu+2)} + \frac{\beta^2}{(\nu+1)}\right]. \quad (17)$$

For a planar geometry (ν=0), this integral leads to the same contribution to the free energy ($\sim -h^3/3$) as that from a corresponding term of Equation (40) of ref. [31].

Equilibrium W^{el} gives the coupled electrostatic-energy and elasticity contributions to the gel free energy. At small $R\kappa\gamma$, the square bracket of Equation (16) goes to $2/(\nu+3)$. Provided that the solvent pool is also small compared to the size of the domain shown in Figure 1, γ<<1, Equation (16) is dominated by the second term in parentheses.

For $R\kappa\gamma$>>1, corresponding to a gel with large solvent pools at nonvanishing external salinity, Equation (16) can be expanded in powers of $(R\kappa\gamma)^{-1}$:

$$\frac{W^{el}}{RA(R)} = \frac{1}{2\pi l_B H_0^2}\left\{\frac{h^2}{2R\kappa}\gamma^{\nu}\left[1 - \frac{\nu(\nu+2)}{8}\frac{1}{(R\kappa\gamma)^2}\right] + \frac{R^2}{H_0^2} I_A(\beta,\gamma)\right\}. \quad (18)$$

For nonplanar geometries, this equation represents the curvature expansion of W^{el}. At large *R*, this equation is also dominated by the second term in parentheses.

Putting together different contributions to the free energy, Equations (1, 14, 16), we finally write for the equilibrium Helmholtz energy:

$$\frac{F^{gel}}{RA(R)} = \sigma_{AB}\frac{a(\beta)}{R} + \frac{F^{mix}_{nonel}}{RA(R)} + (\lambda_+ - 1)\left[\bar{c}_s - \alpha\bar{c}_p\right]\mathrm{v}(\beta) + (\lambda_- - 1)\bar{c}_s\mathrm{v}(\beta) +$$

$$+ \Psi_I(\beta)\alpha\bar{c}_p\mathrm{v}(\beta) - \frac{W^{el}}{RA(R)} + \frac{R^2 B_B I_B(\beta)}{a_K^3} \quad (19)$$

where F^{mix}_{nonel} is calculated from the Flory-Huggins expression; $\bar{c}_s$ is the average concentration of salt; and $\bar{c}_p$ is the average concentration of polymer within the A-domain of the gel:

$$\bar{c}_s = \frac{1}{\mathrm{v}(\beta)} \int_0^{\beta} \rho_-(y) a(y) dy \tag{20}$$

$$\bar{c}_p = \frac{1}{\mathrm{v}(\beta)} \int_0^{\beta} c_p(y) a(y) dy \,. \tag{21}$$

The integral $I_B(\beta)$ in Equation (19) describes the elastic response of B-blocks [37, 38]:

$$I_B(\beta) = \int_{\beta}^{1} (\beta - y)^2 a(y) dy = \frac{1}{(\nu+3)} - \frac{2\beta}{(\nu+2)} + \frac{\beta^2}{(\nu+1)} - \frac{2\beta^{\nu+3}}{(\nu+3)(\nu+2)(\nu+1)} \,. \tag{22}$$

The electric potential at the A-B interface, $\Psi_I(\beta)$, is found from the condition of continuity of the potential at the free end of the swollen brush ($y = \gamma$):

$$\Psi_I(\beta) = h^2 + \Psi_{II}(\gamma) = h^2 + \frac{2h}{H_0 \kappa} \frac{I_{z-1}(R\kappa\gamma)}{I_z(R\kappa\gamma)} \,. \tag{23}$$

In the derivation of this equation, the potential zero has been chosen in the bulk solution ($\lambda_+ = \lambda_- = \ln c_s^b$). For a strongly swollen gel, Equation (23) reduces to (see Appendix 1):

$$\Psi_I(\beta) \cong h^2 + \frac{2h}{H_0 \kappa} \,. \tag{24}$$

<u>Distribution of Ions and an Equation for the A-Brush Thickness</u>

The distribution of mobile charges within the polymer brush is given by:

$$\rho_+(y) = c_s^b e^{-\Psi_I(\beta)} e^{K(\beta - y)^2} \tag{25}$$

$$\rho_-(y) = c_s^b e^{\Psi_I(\beta)} e^{-K(\beta - y)^2} \tag{26}$$

and the profile of the polymer concentration is:

$$\alpha c_A(y) = \rho_-(y) - \rho_+(y) - \frac{1}{2\pi l_B H_0^2} \left[\frac{\beta - y}{y} \nu - 1 \right] . \tag{27}$$

The A-brush thickness, h, is obtained by calculating the total charge accumulated in the brush. From the Poisson equation we have:

$$\int_{\gamma}^{\beta} \rho(y)a(y)dy = -\frac{1}{4\pi l_B}\int_{\gamma}^{\beta} \nabla^2 \Psi_I(y)a(y)dy = \frac{a(\gamma)(\beta-\gamma)}{2\pi l_B H_0^2}. \tag{28}$$

On the other hand, from the material balance and Boltzmann distribution of mobile charges:

$$\int_{\gamma}^{\beta} \rho(y)a(y)dy =$$

$$= \int_{\gamma}^{\beta} \alpha c_p(y)a(y)dy + \rho_+^0 e^{-\Psi_I(\beta)}\int_{\gamma}^{\beta} e^{K(\beta-y)^2} a(y)dy - \rho_-^0 e^{\Psi_I(\beta)}\int_{\gamma}^{\beta} e^{-K(\beta-y)^2} a(y)dy. \tag{29}$$

Taking into account Equation (23), Equations (28) and (29) together give:

$$ha(\gamma) = \frac{H_0}{\Lambda} + \frac{H_0 R\kappa^2}{4}\left[e^{-h^2} e^{-\Psi_{II}(\gamma)} J_\nu^+ - e^{h^2} e^{\Psi_{II}(\gamma)} J_\nu^-\right] \tag{30}$$

where $\Lambda = \dfrac{A(R)}{2\pi l_B \alpha N_A n_p}$ is the Guoy-Chapmann length corresponding to the fixed charge of the brush, N_A is the number of segments in the A-subchain; $n_p = \bar{c}_p \mathrm{v}(\beta)A(R)R/N_A$ is the number of polymer chains; and the integrals

$$J_\nu^{\pm} \equiv \int_{\gamma}^{\beta} e^{\pm K(\beta-y)^2} y^\nu dy \tag{31}$$

come from the distribution of the positive and negative mobile charges (Equations (25),(26)) inside the polymer brush. These integrals are related to the Dawson integral and to the error-function integral for a planar case; they can also be estimated for other geometries (see Appendix 2). For the planar case (ν=0), Equation (30) can be compared with the result obtained from the non-linear Poisson-Boltzmann equation by Zhulina et al., [29, 30] for a polyelectrolyte brush immersed in a salt solution. For a very large solvent pool, we may use Equation (24). For small potentials, where the linear approximation to the Poisson-Boltzmann equation is valid, *h* is small. An expansion of the exponential in Equation (30) in powers of *h* and a similar expansion of Equation (18) of reference [29] lead to identical series up to O(h^3).

Equation (30), the result of electroneutrality, is similar to the Donnan relation because it also incorporates the Boltzmann distribution of the mobile charges. However, it is somewhat different from the classical Donnan relation because it incorporates not only the charges immobilized on the polymer chains, but also the total charge of the brush that is determined by the parabolic electric potential within the brush.

Swelling Equilibrium

When the gel is in equilibrium with an outside solution with respect to the distribution of mobile ions, it is convenient to use the semigrand thermodynamic potential defined by:

$$\mathbf{\Omega}^{gel} \equiv F^{gel} - n_+ \mu_+^{bulk} - n_- \mu_-^{bulk} , \tag{32}$$

where n_+ is the total number of positive and n_- is the total number of negative mobile ions in the gel and $\mu_+^{bulk}, \mu_-^{bulk}$ are their equilibrium chemical potentials. We use the same reference chemical potential for an ion in the gel and in the outside solution, consistent with the assumption that the dielectric constants of these two media are the same. Applying excess quantities, we write λ_+ instead of μ_+^{bulk} and λ_- instead of μ_-^{bulk}. To find the equilibrium structure of the gel, more specifically, the equilibrium size R of the domains of a given morphology, we seek a minimum of Ω^{gel} per unit volume with respect to R. The minimum desired is at fixed λ_+, λ_- and at fixed swelling expressed as average fraction of solvent in the gel. The equilibrium swelling is found by equating the osmotic pressure inside the gel to that in the outside solution:

$$\Pi^{gel} \equiv -\left(\frac{\partial \Omega^{gel}}{\partial V} \right)_{T, n_p, \lambda_+, \lambda_-} = \Pi^{bulk} . \tag{33}$$

For an incompressible system (and point-charge ions), Equation (33) coincides with the requirement of the equality of the solvent chemical potential because $\frac{\partial}{\partial V} = \frac{1}{a_K^3} \frac{\partial}{\partial n_s}$ at

$n_p = const$, where n_s is the number of solvent molecules [24]. We now turn to the derivation of equations that determine the internal (domain size) and the external (swelling) equilibria of the gel.

The gel free energy depends on domain size *R*, and on the positions of boundaries γ and β (see Equations (16), (19), (23) and (32)). The dependence on the extent of swelling can also be expressed via β. If, for example, φ_s is the average volume fraction of solvent in the gel, then:

$$f_B(1-\varphi_s) = 1-\beta^{\nu+1} \tag{34}$$

where $f_B = 1 - f_A = N_B/(N_B + N_A)$ gives the composition asymmetry of the block-copolymer chain. At fixed swelling (β), the domain size (R) and the pool size (γ) are related through Equation (30) that incorporates the electroneutrality condition. Hence we have a constrained minimization problem when searching for the equilibrium size:

$$\min_{\{R\}} g^{gel}(R,\gamma) \tag{35}$$

where $g^{gel} = \dfrac{\mathbf{\Omega}^{gel}}{R\boldsymbol{A}(R)}$ and R is related to γ by Equation (30). The necessary condition of the minimum is:

$$\left(\frac{\partial g^{gel}}{\partial R}\right)_\gamma + \left(\frac{\partial g^{gel}}{\partial \gamma}\right)_R \left(\frac{\partial \gamma}{\partial R}\right) = 0\,. \tag{36}$$

Using Equations (19, 32), Equation (36) can be rewritten as:

$$-\frac{\sigma_{AB}a(\beta)}{R^2} + 2R\frac{B_B I_B(\beta)}{a_K^3} + \alpha\bar{c}_p \mathrm{v}(\beta)\left[\frac{\partial \mathbf{\Psi}_I(\beta)}{\partial R} + \frac{\partial \mathbf{\Psi}_I(\beta)}{\partial \gamma}\frac{\partial \gamma}{\partial R}\right] +$$

$$+\frac{\partial}{\partial R}\left[\frac{F^{mob}}{R\boldsymbol{A}(R)} - \frac{W^{el}}{R\boldsymbol{A}(R)}\right] + \frac{\partial}{\partial \gamma}\left[\frac{F^{mob}}{R\boldsymbol{A}(R)} - \frac{W^{el}}{R\boldsymbol{A}(R)} + \frac{F^{mix}_{nonel}}{R\boldsymbol{A}(R)}\right]\left(\frac{\partial \gamma}{\partial R}\right) = 0 \tag{37}$$

where

$$\frac{F^{mob}}{RA(R)} = -\int_0^{\beta} \rho_+(y)a(y)dy - \int_0^{\beta} \rho_-(y)a(y)dy =$$

$$= -c_s^b \left[2\mathrm{v}(\gamma) + e^{-\Psi_I(\beta)} J_v^+ + e^{\Psi_I(\beta)} J_v^- \right] \tag{38}$$

is determined by the total number of mobile charges in the gel and W^{el} is given by Equation (16). All terms in Equation (37) are expressed analytically (Appendix 3). The derivative $\partial\gamma/\partial R$ is found from a linear equation that is obtained by differentiating Equation (30) with respect to R.

At a given solvent fraction inside the gel (extent of swelling β), the equilibrium domain size (R) and solvent-pool boundary (γ) are determined by solving Equations (37) and (30) simultaneously. The equilibrium swelling is then found by searching for the solvent fraction that satisfies Equation (33). For the 1:1 salt considered in this work, the osmotic pressure outside the gel is given by:

$$\Pi^{bulk} = 2c_s^b . \tag{39}$$

The osmotic pressure inside the gel is expressed analytically as a sum of several contributions:

$$\Pi^{gel} = \Pi^{surf} + \Pi_{nonel}^{mix} + \Pi^{el} + \Pi^{poly} + \Pi^{mob} + \Pi_B^{str} + \Pi^{\gamma} . \tag{40}$$

A similar expression for the chemical potential $\mu_{solv}^I = -a_K^3 \Pi^{gel}$ is given in Appendix 4. The first six terms in the right-hand side of Equation (40) come directly from the dependence on the solvent uptake of different contributions to the gel free energy. Analytical expressions for these terms are given in Appendix 5. The first two terms of Equation (40), Π^{surf} and Π_{nonel}^{mix}, describe the contributions to the osmotic pressure from the bare interface between the A- and B-microdomains and from the mixing of A-subchains with solvent, respectively. The electrostatic effects coupled with the elasticity of the swollen A-brush are reflected by Π^{el}, Π^{poly} and Π^{mob}, where Π^{el} contains contributions from weighted electrostatic and elastic energy; Π^{poly}

is determined by the electric potential at the boundary between the hydrophobic and hydrophilic copolymer domains, and Π^{mob} describes the contribution of the mobile ions inside the gel to osmotic pressure. Π_B^{str} is determined by the elasticity of the hydrophobic B-subchains. The last term, Π^{γ}, comes from the dependence of the gel free energy on the size of the solvent pool γ that depends, in turn, on the solvent uptake. Π^{γ} is defined in Appendix 4 by Equations (A4.3),(A4.4) and contains electrostatic and mixing contributions. The derivatives that enter these latter equations are calculated analytically as explained in Appendix 3 (Equations (A3.2), (A3.5), (A3.8), (A3.12) and (A3.14)).

Calculated results

Our model gives thermodynamic functions for a swollen ionic gel in terms of modified Bessel functions and special functions $J_{\nu}^{\pm}$ that can be evaluated readily (Appendix 2). In addition to the molecular parameters for a non-ionic gel [37, 38] (chain length N, flexibility a_K, copolymer composition f_A, polymer-polymer and polymer-solvent interaction parameters χ_{AB}, χ_{AS}), the gel degree of ionization α should be specified. The dimensionless size of the pool inside the microdomains (γ) is found from the electroneutrality condition, Equation (30). The microdomain spacing (*R*) is obtained from the condition of internal equilibrium, Equation (37). Equilibrium of the gel with the outside solution of salt is expressed by Equation (33). However, an attempt to find equilibrium swelling shows that the gel has an infinite tendency to swell for all morphologies considered in this work. This is a natural consequence of the repulsion of overlapping electrical double layers inside the solvent pools. Within the proposed model, equilibrium swelling can only be found if we require that upon forming microdomains of a given

morphology at certain solvent content, the gel does not reassemble freely. Starting from this specified solvent fraction φ_s^* (e.g., from the microphase transition point or some other φ_s^*), the size of the microdomain is determined by how much solvent is added. This is equivalent to considering entanglements of polymer chains (or some effective cross-links) that prevent the polymer chains from leaving a microdomain and accumulating in another one. The fraction of solvent in the gel, φ_s^*, at the point where we last allow free self-assembly of the gel can be considered as the solvent fraction at preparation. For $\varphi_s > \varphi_s^*$ we no longer minimize the gel free energy with respect to *R*. Instead, *R* is calculated from an additional packing constraint, Equation (A3.4) that assumes constancy of the number of chains per unit area in the lamellae, per unit length of the long axis in the cylinders and per one domain in the spheres. Hence at $\varphi_s > \varphi_s^*$ the derivative of the gel free energy with respect to *R* is no longer equal to zero leading to additional terms in the expressions for the chemical potential (See Appendix 4 for details). As a result, finite equilibrium swelling is predicted by the model for gels of bicontinuous, cylindrical and spherical morphologies. For a lamellar gel, addition of solvent leads to saturation of the hydrophilic brush; upon reaching saturation, the thickness of an A- or B- lamellar layers does not change and all added solvent goes to the pool. Similar behavior has been predicted in modeling nonionic lamellar gels [37, 38]. However, for an ionic lamellar gel, electrostatic repulsion results in infinite equilibrium swelling. Because the compensating action of dispersion forces across the solvent pool is not included in our model, it always predicts spontaneous breakup for an ionic lamellar gel in the outside solution.

Figures 2 and 3 give structural details calculated for a swollen gel: the distribution of mobile ions, the fixed charge, and the electrical potential within the microdomain. Figure 2 shows screening of the brush charge at high salt concentration. The solution inside the pool is almost identical to the bulk solution. Figure 3 is for low salt concentration. The coions fail to penetrate

the polymer brush. At the same time, the charge imbalance inside the brush is stronger for the low-salt case. The solvent pool feels the presence of the charged brush, and the ionic composition of the pool deviates from that in the bulk solution. In both Figure2 and Figure 3 the electric potential at the polymer-solvent pool boundary is less than 25mV, justifying application of the linearized Poisson-Boltzmann equation for the pool.

Comparison with experimental results Numerous data on equilibrium swelling [6-9, 12,13] are available reflecting the effects of salt, crosslinking density, fraction at preparation and ionic charge of the gel. Microphase-separated ionic gels have also been studied [9]. Unfortunately, to the best of our knowledge, there are no sufficiently detailed data for simultaneous comparison of thermodynamic properties and structural characteristics of microphase-separated diblock-copolymer ionic gels of different morphologies. Therefore, our comparison is limited to a discussion of general trends.

Calculation of equilibrium swelling is illustrated in Figure 4. This figure gives the chemical potential of solvent in the gel in excess of that in the outside solution versus solvent uptake. Equilibrium uptake corresponds to the zero of the excess chemical potential. For $\varphi_s \le \varphi_s^* = 0.91$ free self-assembly of the gel is allowed and the excess chemical potential is calculated with the aid of Equation (40) as explained in Appendix 4, case I, using expressions of Appendix 5 for different terms of the osmotic pressure. For $\varphi_s > 0.91$ frozen entanglements become effective and extra terms are added to the excess chemical potential as explained in Appendix 4, case II. Before continuing to discuss the results of Figure 4 we report some of our general observations on equilibrium swelling.

According to our calculations, an increase of ionic charge of the gel leads to increased swelling. Thus ionic gels swell more than nonionic gels [37, 38] composed of similar polymer chains, in agreement with experiment. Equilibrium swelling for ionic gels of different

morphology changes in the sequence: lamellae (gel breakup) > bicontinuous > cylinders > spheres. The same trend for swelling is predicted by the model for nonionic gels with swollen inner domains and no pools [38]. The difference in equilibrium swelling for different shapes is substantial, particularly at low salt concentrations. Addition of salt screens interaction between the electrical double layers in the pool and diminishes the effect of shape on equilibrium swelling as illustrated in Figure 4. Unusual results are obtained for lamellar gels that have infinite tendency for swelling. At high salt concentration, screening can be so strong that the excess negative value of the solvent chemical potential becomes vanishingly small at a moderate solvent uptake (while remaining negative at all solvent contents of the gel). This situation is illustrated in Figure 4 for a weakly charged gel. Thermal fluctuations may prevent a lamellar ionic gel from reaching true equilibrium in a finite time; at high salt concentrations, this gel may behave similar to a nonionic lamellar gel that has finite swelling. Thus our model suggests that the swelling observed for an ionic lamellar gel (e.g., in overnight swelling) may well be less than that for spherical or cylindrical gels.

Figure 5 shows the effects of ionic charge and assumed shape of the gel microdomains on the calculated swelling pressure. The swelling pressure is equal to the osmotic pressure in the gel in excess of that in the outside solution. It is calculated as explained in Appendix 4, case II, using equations of Appendix 5. For all solvent uptakes given in Figure 5, $\varphi_s > \varphi_s^*$. Zero swelling pressure corresponds to equilibrium swelling of the gel. To estimate the magnitude and scaling of swelling pressure with a solvent uptake typical of hydrogels, experimental data on a chemically crosslinked sodium polyacrylate hydrogel [12] are also shown in Figure 5.

Figure 6 shows predicted equilibrium swelling versus salt content of the bulk solution. Also shown are results obtained by combining the Flory-Rehner theory with that of Donnan. In applying this classical combination, all mixing, electrostatic, and chain-stretching effects are

attributed to the A-domains of the gel. The solvophobic B-domains are assumed to play the role of effective cross-links. Thus equilibrium swelling is calculated from:

$$\frac{\phi_A^*}{N_c}\left[\left(\frac{\phi_A}{\phi_A^*}\right)^{1/3}-\frac{1}{2}\left(\frac{\phi_A}{\phi_A^*}\right)\right]+\ln(1-\phi_A)+\phi_A+\chi_{AS}\phi_A^2-2a_K^3c_s^b\left[\left(\left(\frac{\alpha\phi_A}{2a_K^3c_s^b}\right)^2+1\right)^{1/2}-1\right]=0 \quad (41)$$

where ϕ_A is the average volume fraction of A-chains in the swollen A-domain; ϕ_A^* is this fraction at preparation of the gel and N_c is the number of elastically active segments in the chain, a key parameter of the theory. At high salt concentration the last bracket of Equation (41) reduces to a term that is quadratic in ϕ_A and the only effect of electrostatic interactions is to change the effective value of the Flory-Huggins parameter to $\left[\chi_{AS}-\frac{\alpha^2}{4a_K^3c_s^b}\right]$ [47]. To compare the effect of salt on equilibrium swelling predicted by our model with that predicted by Equation (41), parameter N_c has been adjusted to reproduce approximately the equilibrium swelling of gels calculated with the aid of our model in the limit of high salt concentration; see Figure 6. At low salt concentration and high ionic charge, the equilibrium swelling given by the classical theory lies between the results calculated using our model for cylindrical and bicontinuous gels. For weakly charged gels, the sequence of predicted curves changes, as shown in Figure 6. We demonstrate the effects that can be reproduced by the classical Flory-Rehner+Donnan theory, [10, 14] viz., an increase of swelling with the ionic charge of the gel and shrinking of the gel upon addition of salt. Similar to the classical Flory-Rehner+Donnan theory, our model does not predict an upturn of swelling upon further increase of salt concentration. However, we show a new feature of our model: equilibrium swelling substantially depends on the morphology of a microphase-separated gel. Thus, in this work we derived a simplified analytical model that accounts for the effect of gel mesostructure on its swelling behavior. Because in this work we do

not take into account charge regulation, we do not account for shrinking of the gel at very low salt concentration. Introduction of an ionization-equilibrium constant would give shrinkage as given in the classical theory.

Conclusion

We have developed a model for the equilibrium properties of a diblock copolymer ionic gel swollen in a univalent salt solution using self-consistent field theory. We made a number of simplifying assumptions: strong segregation of block-copolymer fragments; dominance of electrostatics in determining the structural arrangement of polymer subchains; neglect of the packing frustration. These simplifications lead to analytical results for gels of lamellar, bicontinuous, cylindrical and spherical morphologies. The model gives explicit expressions for the gel free energy and for the osmotic pressure in terms of modified Bessel functions, some other special functions related to the Dawson integral and to the error-function integral, and the characteristic size of the microdomains.

The gel molecules are characterized by specifying the chain composition, length, flexibility, the degree of ionization, and by effective polymer-polymer and polymer-solvent interaction parameters. The solvent fraction at preparation of the gel is introduced as the solvent fraction at which the polymer chains freely self-assemble and form microdomains of equilibrium size.

A preliminary test of the model for gels of varying ionic charge swollen in solutions of varying salinity indicates promising results. The model describes a number of complex effects on gel-swelling behavior including those from ionic charge, salt concentration, gel morphology, solvent fraction at preparation of the gel, copolymer chain flexibility and gel composition. Apart from the well-known increase of swelling with ionic charge and the shrinking of a gel upon addition of salt, the model describes the dependence of gel behavior on its morphology. In

comparison with classical Flory-Rehner theory, this prediction is a novelty. The model gives reasonable microdomain spacing and details of gel structure, including spatial distribution of mobile ions and polymer segments, and the electrical potential across the microdomains.

The model expressions can be extended in a straightforward manner to symmetric *z:z* electrolytes.

Acknowledgements

For financial support the authors are grateful to the Office for Basic Sciences of the US Department of Energy, to Bausch and Lomb, Rochester, New York; to Ciba-Vision Corporation, Duluth, Georgia; and to the Russian Foundation for Basic Research (Project #05-03-33267).

Appendix 1

Solution of the linearized Poisson-Boltzmann equation for the polymer-free zone inside the swollen gel

Solutions of the Poisson-Boltzmann equation for a double electric layer of planar, spherical and cylindrical symmetry are well known [39, 48-53]. However, to the best of our knowledge, bicontinuous structures have not previously been considered.

Linearizing the Poisson-Boltzmann equation for the solvent pool, Equation (9), and expressing the Laplacian by Equations (13, 4), we obtain:

$$\frac{\partial^2 \Psi_{II}}{\partial y^2} + \frac{\nu}{y}\frac{\partial \Psi_{II}}{\partial y} = R^2\kappa^2\left[\Psi_{II} + C\right] \tag{A1.1}$$

where $\kappa^2 = 4\pi l_B\left[\rho_+^0 + \rho_-^0\right]$, $C = \left[\rho_-^0 - \rho_+^0\right]/\left[\rho_-^0 + \rho_+^0\right]$ and ν=0, ½, 1, 2 for lamellar, bicontinuous, cylindrical and spherical morphology, respectively.

Constant C can be set equal to zero by setting the potential equal to zero in the bulk phase, whence $\rho_-^0 = \rho_+^0 = c_s^b$ where c_s^b is the concentration of 1:1 salt in the bulk solution. Then κ^{-1} is equal to the usual Debye screening length: $\kappa^2 = 8\pi l_B c_s^b$. Equation (A1.1) becomes homogeneous; using a substitution $\theta = y^{\nu/2}\Psi_{II}$, it can be rewritten as:

$$\theta'' + \left[\frac{1}{y^2}\frac{\nu}{2}\left(1 - \frac{\nu}{2}\right) - R^2\kappa^2\right]\theta = 0\,. \tag{A1.2}$$

This equation is solved by the Frobenius power-series technique (see [54], page 519) where the solution of the indicial equation ($k = \nu/2$) has been chosen to satisfy the boundary condition at the center of the pool; the potential must be a symmetric function of *y*. This leads to a potential of the form:

$$\Psi_{II} = a_0 \Gamma(z) \left(\frac{R\kappa y}{2} \right)^{1-z} \sum_{s=0} \frac{1}{s!(s+z-1)!} \left(\frac{R\kappa y}{2} \right)^{2s+z-1} =$$

$$= a_0 \Gamma(z) \left(\frac{R\kappa y}{2} \right)^{1-z} I_{z-1}(R\kappa y) \qquad \text{(A1.3)}$$

where $z = (\nu + 1)/2$; $\Gamma(z)$ is the gamma function and $I_{z-1}(R\kappa y)$ is the modified Bessel function of order *z-1* (see [54], page 708).

For a planar geometry and for spheres, the *y*-dependence in the brackets of Equation (A1.2) vanishes and we obtain the well-known solutions expressed via the hyperbolic sine, $\Psi_{II}^{plane} \sim \sinh y$, and $\Psi_{II}^{sph} \sim \frac{1}{y} \sinh y$.

Constant a_0 in Equation (A1.3) is determined from the second boundary condition, Equation (12), which gives:

$$\Psi_{II}(y) = \frac{2h}{H_0 \kappa} \left(\frac{y}{\gamma} \right)^{1-z} \frac{I_{z-1}(R\kappa y)}{I_z(R\kappa\gamma)}. \qquad \text{(A1.4)}$$

For a highly swollen gel (large $R\kappa\gamma$) the potential at the edge of the polymer brush, $y = \gamma$, can be found from the asymptotic expansions of the Bessel functions (see [54], page 718) giving:

$$\Psi_{II}(y = \gamma) = \frac{2h}{H_0 \kappa} \left(1 + \frac{\nu}{2} \frac{1}{R\kappa\gamma} + \frac{\nu}{4} \left(1 + \frac{\nu}{2} \right) \frac{1}{(R\kappa\gamma)^2} + \ldots \right). \qquad \text{(A1.5)}$$

Equation (A1.5) represents the potential at the polymer surface as a power series in the curvature. The planar-case limit is $\Psi_{II}(y = \gamma) \to 2h/(H_0 \kappa)$ and corresponds to a large separation of lamellar brushes with non-overlapping double electric layers.

Because $\left(I_{z-1}(x)/I_z(x)\right)_{x\to 0} \to (\nu+1)/x$, the potential given by Equation (A1.4) diverges at small γ:

$$\Psi_{II}(y=\gamma) \to \frac{2h}{H_0\kappa}\frac{(\nu+1)}{R\kappa\gamma} \tag{A1.6}$$

This divergence follows from the tacit assumption that there is always some uncompensated charge within the brush leading to repulsion between the brush edges and formation of the solvent pool. With the parabolic potential, the electric field at the edge of the brush never vanishes and requires the presence of a solvent pool with some compensating charge.

Appendix 2

Integration of the distribution of mobile charges within the brush

We need to estimate integrals of the form:

$$J_\nu^+ \equiv \int_\gamma^\beta e^{K(\beta-y)^2} y^\nu dy \tag{A2.1}$$

and

$$J_\nu^- \equiv \int_\gamma^\beta e^{-K(\beta-y)^2} y^\nu dy\,. \tag{A2.2}$$

For ν=0,1,2 these integrals can be related to the error function and to the Dawson (see Appendices 6 and 8 of ref.25) integrals. However, for a bicontinuous structure we need the integrals at ν=1/2. For integer ν=0,1,2,… $J_\nu^\pm$ are computed using the following integrals:

$$I_\nu^\pm \equiv \int_0^h e^{\pm t^2} t^\nu dt \tag{A2.3}$$

where $h = R(\beta - \gamma)/H_0$. At ν=0 these latter integrals are related to the Dawson integral, $Daws(h) = e^{-h^2}\int_0^h e^{t^2}dt$, and to the error-function integral, $erf(h) = \frac{2}{\sqrt{\pi}}\int_0^h e^{-t^2}dt$, in the following way:

$$I_0^+ = e^{h^2} Daws(h) \tag{A2.4}$$

$$I_0^- = \frac{\sqrt{\pi}}{2} erf(h). \tag{A2.5}$$

At ν=1 straightforward integration of Equation (A2.3) gives:

$$I_1^\pm = \pm\frac{1}{2}\left(e^{\pm h^2} - 1\right). \tag{A2.6}$$

Integration of Equation (A2.3) by parts results in the following recursion relation for ν=2,3,4,…:

$$I_{\nu+2}^\pm = \pm\frac{1}{2}\left[e^{\pm h^2} h^{\nu+1} - (\nu+1) I_\nu^\pm\right]. \tag{A2.7}$$

Following some algebra we find expressions for $J_\nu^\pm$:

$$\begin{aligned}
J_0^\pm &= \frac{1}{K^{1/2}} I_0^\pm, \\
J_1^\pm &= \frac{\beta}{K^{1/2}} I_0^\pm - \frac{1}{K} I_1^\pm, \\
J_2^\pm &= \frac{\beta^2}{K^{1/2}} I_0^\pm - \frac{2\beta}{K} I_1^\pm + \frac{1}{K^{3/2}} I_2^\pm, \\
J_3^\pm &= \frac{\beta^3}{K^{1/2}} I_0^\pm - \frac{3\beta^2}{K} I_1^\pm + \frac{3\beta}{K^{3/2}} I_2^\pm - \frac{1}{K^2} I_3^\pm, \\
J_4^\pm &= \frac{\beta^4}{K^{1/2}} I_0^\pm - \frac{4\beta^3}{K} I_1^\pm + \frac{6\beta^2}{K^{3/2}} I_2^\pm - \frac{4\beta}{K^2} I_3^\pm + \frac{1}{K^{5/2}} I_4^\pm,
\end{aligned} \tag{A2.8}$$

$$J_5^{\pm} = \frac{\beta^5}{K^{1/2}} I_0^{\pm} - \frac{5\beta^4}{K} I_1^{\pm} + \frac{10\beta^3}{K^{3/2}} I_2^{\pm} - \frac{10\beta^2}{K^2} I_3^{\pm} + \frac{5\beta}{K^{5/2}} I_4^{\pm} - \frac{1}{K^3} I_5^{\pm},$$

where $K = (R/H_0)^2$. The coefficients in Equation (A2.8) come from the binomial series. Six integrals above suffice to calculate all thermodynamic properties and their deriatives for lamellae, cylinders and spheres. Cubic interpolation of the integrals (A2.8) has been used to estimate the integrals needed for bicontinuous structure, viz., $J_{1/2}^{\pm}$, $J_{3/2}^{\pm}$, and $J_{5/2}^{\pm}$.

At low swelling, another robust technique for estimating (A2.1) and (A2.2) can be used. Integrating (A2.1) and (A2.2) by parts, we obtain the recursion relations between the integrals of consecutive order:

$$(\nu+1)J_\nu^+ = \beta^{\nu+1} - \gamma^{\nu+1} e^{K(\beta-\gamma)^2} + 2K\left[\beta J_{\nu+1}^+ - J_{\nu+2}^+\right] \tag{A2.9}$$

$$(\nu+1)J_\nu^- = \beta^{\nu+1} - \gamma^{\nu+1} e^{-K(\beta-\gamma)^2} - 2K\left[\beta J_{\nu+1}^- - J_{\nu+2}^-\right]. \tag{A2.10}$$

At large enough ν we have $J_{\nu+1}^+ \approx J_{\nu+2}^+ \approx 0$ and $J_{\nu+1}^- \approx J_{\nu+2}^- \approx 0$, because $y < 1$. Fixing some large ν and calculating $J_\nu^{\pm}, J_{\nu-1}^{\pm}, J_{\nu-2}^{\pm}, J_{\nu-3}^{\pm}, \ldots$, by the recursion relations (A2.9-A2.10) we eventually obtain a numerical estimate for $J_2^{\pm}, J_1^{\pm}, J_0^{\pm}$ or $J_{5/2}^{\pm}, J_{3/2}^{\pm}, J_{1/2}^{\pm}$. This procedure has been tested by calculating the error function and the Dawson integral (starting from ν=120). Up to 7-9 significant figures, the results are identical to those obtained by standard routines from the Fortran-IMSL library. As indicated by Equations (A2.1, A2.2), the integrals for noninteger ν lie between consecutive integrals for the integers, e.g.: $J_1^{\pm} < J_{1/2}^{\pm} < J_0^{\pm}$. Typically, the exponent $K(\beta-\gamma)^2 = 3\pi^2 R^2 (\beta-\gamma)^2 / (8\alpha N_A^2 a_K^2)$ is not large ($\sim N_A^{-1}\alpha^{-1}$ for a Gaussian chain). When it becomes substantial for a fully-extended chain ($\sim\alpha^{-1}$), convergence becomes a problem. In this case the integrals $J_\nu^{\pm}$ were estimated with the aid of Equations (A2.8).

Appendix 3

Expressions for the derivatives in the condition of internal equilibrium of the gel, Equation (37)

Expressions for the derivatives of the electric potential at the boundary are found from Equation (23):

$$\frac{\partial \Psi_I(\beta)}{\partial R} = \frac{1}{R}\left[h^2 + \Psi_I(\beta)\right] + \frac{2h\gamma}{H_0}\frac{\partial\left(I_{z-1}(x)/I_z(x)\right)}{\partial x} \tag{A3.1}$$

and

$$\frac{\partial \Psi_I(\beta)}{\partial \gamma} = -\frac{R}{H_0 h}\left[h^2 + \Psi_I(\beta)\right] + \frac{2hR}{H_0}\frac{\partial\left(I_{z-1}(x)/I_z(x)\right)}{\partial x} \tag{A3.2}$$

where the derivatives of the modified Bessel functions with respect to $x = R\kappa\gamma$ are given by:

$$\frac{\partial\left(I_{z-1}/I_z\right)}{\partial x} = 1 - \frac{I_{z-1}}{I_z}\left[\frac{I_{z-1}}{I_z} - \frac{\nu}{x}\right]. \tag{A3.3}$$

From Equation (16) we have:

$$\frac{\partial}{\partial R}\left[\frac{W^{el}}{RA(R)}\right] = \frac{2W^{el}}{R^2 A(R)} + \frac{h^2\gamma^{\nu+2}\kappa}{4\pi l_B H_0^2} D \tag{A3.4}$$

and

$$\frac{\partial}{\partial \gamma}\left[\frac{W^{el}}{RA(R)}\right] = \frac{h^2\gamma^{\nu}}{2\pi l_B H_0^2}\left\{\left[1 - \frac{I_{z-1}I_{z+1}}{I_z^2}\right]\left[\frac{\nu+1}{2} - \frac{\gamma}{\beta-\gamma}\right] + \frac{R\kappa\gamma}{2}D - 1\right\} \tag{A3.5}$$

where

$$D = -\frac{\partial\left(I_{z-1}I_{z+1}/I_z^2\right)}{\partial x} = 2\frac{I_{z-1}}{I_z}\left[\left(\frac{I_{z-1}}{I_z}\right)^2 + \frac{I_{z-1}}{I_z}\frac{(1-3z)}{x} + \frac{2z(z-1)}{x^2} - 1\right] + \frac{2z}{x}. \tag{A3.6}$$

Equation (38) gives:

$$\frac{\partial}{\partial R}\left[\frac{F^{mob}}{RA(R)}\right]=-c_s^b\left\{\left[e^{\Psi_I(\beta)}J_\nu^- - e^{-\Psi_I(\beta)}J_\nu^+\right]\frac{\partial\Psi_I(\beta)}{\partial R}+e^{\Psi_I(\beta)}\frac{\partial J_\nu^-}{\partial R}+e^{-\Psi_I(\beta)}\frac{\partial J_\nu^+}{\partial R}\right\} \quad \text{(A3.7)}$$

and

$$\frac{\partial}{\partial \gamma}\left[\frac{F^{mob}}{RA(R)}\right]=-c_s^b\left\{\left[e^{\Psi_I(\beta)}J_\nu^- - e^{-\Psi_I(\beta)}J_\nu^+\right]\frac{\partial\Psi_I(\beta)}{\partial \gamma}+a(\gamma)\left[2-e^{\Psi_I(\beta)-h^2}-e^{-\Psi_I(\beta)+h^2}\right]\right\} \quad \text{(A3.8)}$$

where the derivatives of the integrals $J_\nu^\pm$ are obtained from their definition, Equation (31):

$$\frac{\partial J_\nu^+}{\partial R}=\frac{2R}{H_0^2}\left[\beta^2 J_\nu^+ - 2\beta J_{\nu+1}^+ + J_{\nu+2}^+\right] \quad \text{(A3.9)}$$

and

$$\frac{\partial J_\nu^-}{\partial R}=-\frac{2R}{H_0^2}\left[\beta^2 J_\nu^- - 2\beta J_{\nu+1}^- + J_{\nu+2}^-\right]. \quad \text{(A3.10)}$$

Using the Flory-Huggins equation for nonelectrostatic contribution to the free energy, we have:

$$\frac{F_{nonel}^{mix}a_K^3}{RA(R)}=\left[\mathrm{v}(\beta)-\mathrm{v}(\gamma)\right]\left[\phi_s^A\ln\phi_s^A+\chi_{AS}\phi_s^A(1-\phi_s^A)\right] \quad \text{(A3.11)}$$

where $\phi_s^A=\left[\varphi_s\mathrm{v}(1)-\mathrm{v}(\gamma)\right]/\left[\mathrm{v}(\beta)-\mathrm{v}(\gamma)\right]$ is the average volume fraction of solvent inside the swollen A-brush, and φ_s is the volume fraction of solvent in the gel. Differentiating Equation (A3.11) and performing algebra we obtain:

$$\frac{\partial}{\partial \gamma}\left[\frac{F_{nonel}^{mix}a_K^3}{RA(R)}\right]=-a(\gamma)\left[\ln\phi_s^A+1-\phi_s^A+\chi_{AS}(1-\phi_s^A)^2\right] \quad \text{(A3.12)}$$

which is, essentially, the excess surface free energy at the boundary between the polymer brush and the pool, where there is a stepwise change of solvent fraction from 1 to its average value, ϕ_s^A.

Equations (A3.1-A3.11) are analytical expressions in terms of the modified Bessel functions and $J_\nu^\pm$. These expressions are substituted into Equation (37) for the equilibrium domain size.

To find an expression for $\partial\gamma/\partial R$ we differentiate Equation (30) with the result:

$$\frac{\partial\gamma}{\partial R} =$$

$$= \frac{e^{-\Psi_I(\beta)}\frac{\partial J_\nu^+}{\partial R} - e^{\Psi_I(\beta)}\frac{\partial J_\nu^-}{\partial R} - \left[e^{-\Psi_I(\beta)}J_\nu^+ + e^{\Psi_I(\beta)}J_\nu^-\right]\frac{\partial\Psi_I(\beta)}{\partial R}}{\frac{\gamma^{\nu-1}}{2\pi l_B H_0^2 c_s^b}\left[\nu\beta-(\nu+1)\gamma\right]+\gamma^\nu\left[e^{-\Psi_I(\beta)+h^2} - e^{\Psi_I(\beta)-h^2}\right]+\left[e^{-\Psi_I(\beta)}J_\nu^+ + e^{\Psi_I(\beta)}J_\nu^-\right]\frac{\partial\Psi_I(\beta)}{\partial\gamma}}. \quad \text{(A3.13)}$$

The expressions for the derivatives that appear in the right hand side of this equation are calculated by Equations (A3.1-A3.3) and (A3.9-A3.10).

Similarly, for $\partial\gamma/\partial\beta$ (needed for calculating the solvent chemical potential, see Appendix 4) we obtain:

$$\frac{\partial\gamma}{\partial\beta} =$$

$$= \frac{c_s^b\left[e^{-\Psi_I}\frac{\partial J_\nu^+}{\partial\beta} - e^{\Psi_I}\frac{\partial J_\nu^-}{\partial\beta}\right] - c_s^b\left[e^{-\Psi_I}J_\nu^+ + e^{\Psi_I}J_\nu^-\right]\frac{\partial\Psi_I}{\partial\beta} - \frac{\alpha}{a_K^3}\frac{f_A}{f_B}a(\beta) - \frac{a(\gamma)}{2\pi l_B H_0^2}}{\frac{\gamma^{\nu-1}}{2\pi l_B H_0^2}\left[\nu\beta-(\nu+1)\gamma\right]+c_s^b\gamma^\nu\left[e^{-\Psi_I+h^2} - e^{\Psi_I-h^2}\right]+c_s^b\left[e^{-\Psi_I}J_\nu^+ + e^{\Psi_I}J_\nu^-\right]\frac{\partial\Psi_I}{\partial\gamma}}. \quad \text{(A3.14)}$$

Equation (A3.2) and Equations (A5.7)-(A5.9) of Appendix 5 give explicit expressions for the derivatives in the right hand side of Equation (A3.14).

Appendix 4

Derivation of the expressions for the solvent chemical potential in the gel

We first express the solvent chemical potential in terms of the free energy (per unit volume) of the gel microdomain, g^{gel} (see Equation (35)):

$$\mu_{solv} = \left(\frac{\partial \mathbf{\Omega}^{gel}}{\partial n_s}\right)_{T,n_p,\lambda_+,\lambda_-} = g^{gel}\frac{a_K^3}{\mathrm{v}(1)} + R\boldsymbol{A}(R)\left(\frac{\partial g^{gel}}{\partial n_s}\right). \qquad \text{(A4.1)}$$

g^{gel} itself is determined by Equations (19), (32) and (35) and the main difficulty is to obtain the derivative $\left(\frac{\partial g^{gel}}{\partial n_s}\right)$. To do so recall that g^{gel} depends on the solvent content of the gel via β (see Equation (34)) and it also depends on two parameters describing the internal state of the gel: the microdomain spacing, R, and the size of solvent pool, γ.

Thus $g^{gel} = g^{gel}(R,\beta,\gamma)$ and taking into account that R,β and γ are related by Equation (30) we may write:

$$dg^{gel} = \left[\left(\frac{\partial g^{gel}}{\partial R}\right)_{\gamma,\beta} + \left(\frac{\partial g^{gel}}{\partial \gamma}\right)_{R,\beta}\left(\frac{\partial \gamma}{\partial R}\right)\right]dR + \left[\left(\frac{\partial g^{gel}}{\partial \beta}\right)_{R,\gamma} + \left(\frac{\partial g^{gel}}{\partial \gamma}\right)_{R,\beta}\left(\frac{\partial \gamma}{\partial \beta}\right)\right]d\beta. \qquad \text{(A4.2)}$$

We now divide both sides of Equation (A4.2) by δn_s, write explicit expressions for the derivatives in the brackets, substitute the result into Equation (A4.1), and, upon performing all algebra, obtain the desired expression for the solvent chemical potential. There are two different cases however that we will treat separately.

I. If the gel reaches internal equilibrium by adjusting the microdomain size, the first bracket in Equation (A4.2) is zero (see Equation (36)).

From Equations (19), (32), (35) we find:

$$\left(\frac{\partial g^{gel}}{\partial \gamma}\right)_{R,\beta} = \frac{\partial}{\partial \gamma}\left[\frac{F^{mob}}{R\boldsymbol{A}(R)} - \frac{W^{el}}{R\boldsymbol{A}(R)} + \frac{F^{mix}_{nonel}}{R\boldsymbol{A}(R)}\right] + \alpha\bar{c}_p\mathrm{v}(\beta)\frac{\partial \mathbf{\Psi}_I(\beta)}{\partial \gamma} \qquad \text{(A4.3)}$$

where the derivatives are given by Equations (A3.2), (A3.5), (A3.8), (A3.12). $\partial\gamma/\partial\beta$ is calculated from Equation (A3.14). Introducing

$$\Pi^{\gamma} \equiv -\frac{RA(R)}{a_K^3}\left(\frac{\partial g^{gel}}{\partial\gamma}\right)_{R,\beta}\left(\frac{\partial\gamma}{\partial\beta}\right)\left(\frac{\partial\beta}{\partial n_s}\right) = -\frac{1}{a(\beta)}\left[1-\frac{\mathrm{v}(\beta)}{\mathrm{v}(1)}\right]\left(\frac{\partial g^{gel}}{\partial\gamma}\right)_{R,\beta}\left(\frac{\partial\gamma}{\partial\beta}\right) \quad \text{(A4.4)}$$

into Equations (A4.2), (A4.1) and performing very tedious algebra we get Equation (40) of the text for the osmotic pressure (expressions for the first six terms of Equation (40) are derived in Appendix 5).

II. If some entanglements between copolymer chains prevent free redistribution of copolymer molecules between different microdomains, $g^{gel} = g^{gel}(R,\beta,\gamma)$ is no longer at its minimum with respect to R, and there is a contribution to the chemical potential from the first bracket of Equation (A4.2).

The solvent chemical potential inside the gel is given by:

$$\mu_{solv} = \mu_{solv}^{I} + \Delta\mu_{solv} \quad \text{(A4.5)}$$

where μ_{solv}^{I} is the solvent chemical potential in a freely assembled gel, as calculated for case I, and

$$\Delta\mu_{solv} = RA(R)\left[\left(\frac{\partial g^{gel}}{\partial R}\right)_{\gamma,\beta} + \left(\frac{\partial g^{gel}}{\partial\gamma}\right)_{R,\beta}\left(\frac{\partial\gamma}{\partial R}\right)\right]\left(\frac{\partial R}{\partial n_s}\right)_{n_p}. \quad \text{(A4.6)}$$

The square bracket in this equation is identical to the left-hand side of Equations (36),(37). It is calculated explicitly using the equations of Appendix 3. When copolymer molecules do not redistribute between different microdomains of the gel, the microdomain volume is specified by the number of solvent molecules and we have:

$$\left(\frac{\partial V(R)}{\partial R}\right)_{n_p} = a_K^3\left(\frac{\partial n_s}{\partial R}\right)_{n_p} \quad \text{(A4.7)}$$

Using an approximate relation $dV(R) \cong A(R)dR$ together with Equation (A4.7), we rewrite Equation (A4.6):

$$\Delta\mu_{solv} = a_K^3 R\left[\left(\frac{\partial g^{gel}}{\partial R}\right)_{\gamma,\beta} + \left(\frac{\partial g^{gel}}{\partial \gamma}\right)_{R,\beta}\left(\frac{\partial \gamma}{\partial R}\right)\right]. \tag{A4.8}$$

Case I corresponds to a totally free self-assembly of a mesoscopic gel, whereas case II corresponds to some frozen entanglements or effective crosslinks in the gel. The solvent fraction φ_s^* at which such entanglements are first introduced, can be considered a solvent fraction at preparation of the gel. For a given solvent uptake, i.e., given β, minimization of the gel free energy with respect to the domain size, R, has different meanings for different gel morphologies. For a lamellar gel, variation of R affects the number of chains per unit area, $R[1-\beta]/(N_B a_K^3)$. For a cylindrical gel, change of R changes the number of chains per unit length of the cylinder, $\pi R^2[1-\beta^2]/(N_B a_K^3)$. For a spherical structure, R uniquely defines the number of chains in the sphere, $\frac{4}{3}\pi R^3[1-\beta^3]/(N_B a_K^3)$. When there is no self-assembly ($\varphi > \varphi_s^*$), we calculate the microdomain spacing as we add solvent to gels of different geometries assuming constancy of the number of chains per unit area in the lamellae, per unit length of the long axis in the cylinders and per one domain in the spheres:

$$R^{\nu+1} = (R^*)^{\nu+1}\frac{1-\varphi_s^*}{1-\varphi_s} \tag{A4.9}$$

where R^* is the microdomain spacing at preparation of the gel that is found by solving Equation (37).

Appendix 5

Expressions for contributions to osmotic pressure (Π^{surf}, Π^{mix}_{nonel}, Π^{el}, Π^{poly}, Π^{mob}, Π^{str}_{B}), Equation (40)

The contribution from mixing solvent with polymer is calculated from the Flory-Huggins equation taking into account that the solvent pool does not contribute to mixing terms:

$$a_K^3 \Pi^{mix}_{nonel} = -\left[1-\frac{\mathrm{v}(\gamma)}{\mathrm{v}(1)}\right]\left[\ln\phi_s^A + 1 - \phi_s^A + \chi_{AS}\left(1-\phi_s^A\right)^2\right]. \tag{A5.1}$$

Here ϕ_s^A is the average volume fraction of solvent within the A-brush ($y \in [\gamma, \beta]$).

The surface contribution and the elasticity contribution from the B-brush that does not contain the solvent are calculated as discussed elsewhere [37]:

$$\Pi^{surf} = -\frac{\sigma_{AB}}{R}\left\{\frac{a(\beta)}{\mathrm{v}(1)} + \left[1-\frac{\mathrm{v}(\beta)}{\mathrm{v}(1)}\right]\frac{\partial \ln a(\beta)}{\partial\beta}\right\} \tag{A5.2}$$

$$a_K^3 \Pi^{str}_B = -R^2 B_B\left\{\frac{I_B(\beta)}{\mathrm{v}(1)} + \frac{1}{a(\beta)}\left[1-\frac{\mathrm{v}(\beta)}{\mathrm{v}(1)}\right]\frac{\partial I_B(\beta)}{\partial\beta}\right\}. \tag{A5.3}$$

The electrostatic contribution is coupled with the elasticity contribution from the A-brush that carries fixed charge. These contributions are given by:

$$a_K^3 \Pi^{poly} = -\alpha\frac{f_A}{f_B}\left[1-\frac{\mathrm{v}(\beta)}{\mathrm{v}(1)}\right]^2 \frac{\mathrm{v}(1)}{a(\beta)}\left(\frac{\partial\Psi_I(\beta)}{\partial\beta}\right) \tag{A5.4}$$

$$\Pi^{el} = \frac{R^2}{2\pi l_B H_0^4}\left\{\frac{I_A(\beta,\gamma)}{\mathrm{v}(1)} + \frac{1}{a(\beta)}\left[1-\frac{\mathrm{v}(\beta)}{\mathrm{v}(1)}\right]\frac{\partial I_A(\beta,\gamma)}{\partial\beta} + \right.$$

$$\left. + (\beta-\gamma)\gamma^{\nu+1}\left[1-\frac{I_{z-1}(R\kappa\gamma)I_{z+1}(R\kappa\gamma)}{I_z^2(R\kappa\gamma)}\right]\left[\frac{1}{a(\beta)}\left[1-\frac{\mathrm{v}(\beta)}{\mathrm{v}(1)}\right] + \frac{\beta-\gamma}{2\mathrm{v}(1)}\right]\right\} \tag{A5.5}$$

$$\Pi^{mob} = \frac{c_s^b}{\mathrm{v}(1)}\left\{2\mathrm{v}(\gamma) + e^{-\Psi_I(\beta)}J_\nu^+ + e^{\Psi_I(\beta)}J_\nu^- + \right.$$

$$+\frac{\mathrm{v}(1)}{a(\beta)}\left[1-\frac{\mathrm{v}(\beta)}{\mathrm{v}(1)}\right]\left[e^{-\Psi_I(\beta)}\frac{\partial J_\nu^+}{\partial\beta}+e^{\Psi_I(\beta)}\frac{\partial J_\nu^-}{\partial\beta}+\left(e^{\Psi_I(\beta)}J_\nu^- - e^{-\Psi_I(\beta)}J_\nu^+\right)\left(\frac{\partial\Psi_I(\beta)}{\partial\beta}\right)\right]\Bigg\} \quad \text{(A5.6)}$$

where the last equation gives the contribution of the mobile ions inside the gel to osmotic pressure.

In Equation (A5.6), the derivatives that are related to the distribution of the mobile charge are found from Equation (31):

$$\frac{\partial J_\nu^+}{\partial\beta}=a(\beta)+2K\left[\beta J_\nu^+ - J_{\nu+1}^+\right] \quad \text{(A5.7)}$$

$$\frac{\partial J_\nu^-}{\partial\beta}=a(\beta)-2K\left[\beta J_\nu^- - J_{\nu+1}^-\right] \quad \text{(A5.8)}$$

and the derivative of the potential at the A-B boundary is obtained from Equation (23):

$$\frac{\partial\Psi_I(\beta)}{\partial\beta}=\frac{R}{H_0}\left[h+\frac{\Psi_I(\beta)}{h}\right]. \quad \text{(A5.9)}$$

$\frac{\partial I_A(\beta,\gamma)}{\partial\beta}$ and $\frac{\partial I_B(\beta)}{\partial\beta}$ in Equations (A5.3, A5.4) are calculated analytically from Equations (17,22):

$$\frac{\partial I_A(\beta,\gamma)}{\partial\beta}=\frac{2\beta^{\nu+2}}{(\nu+1)(\nu+2)}+2\gamma^{\nu+1}\left[\frac{\gamma}{(\nu+2)}-\frac{\beta}{(\nu+1)}\right] \quad \text{(A5.10)}$$

$$\frac{\partial I_B(\beta)}{\partial\beta}=-\frac{2\beta^{\nu+2}}{(\nu+1)(\nu+2)}-2\left[\frac{1}{(\nu+2)}-\frac{\beta}{(\nu+1)}\right]. \quad \text{(A5.11)}$$

Calculation of contribution Π^γ to the osmotic pressure is explained in Appendix 4, Equation (A4.4).

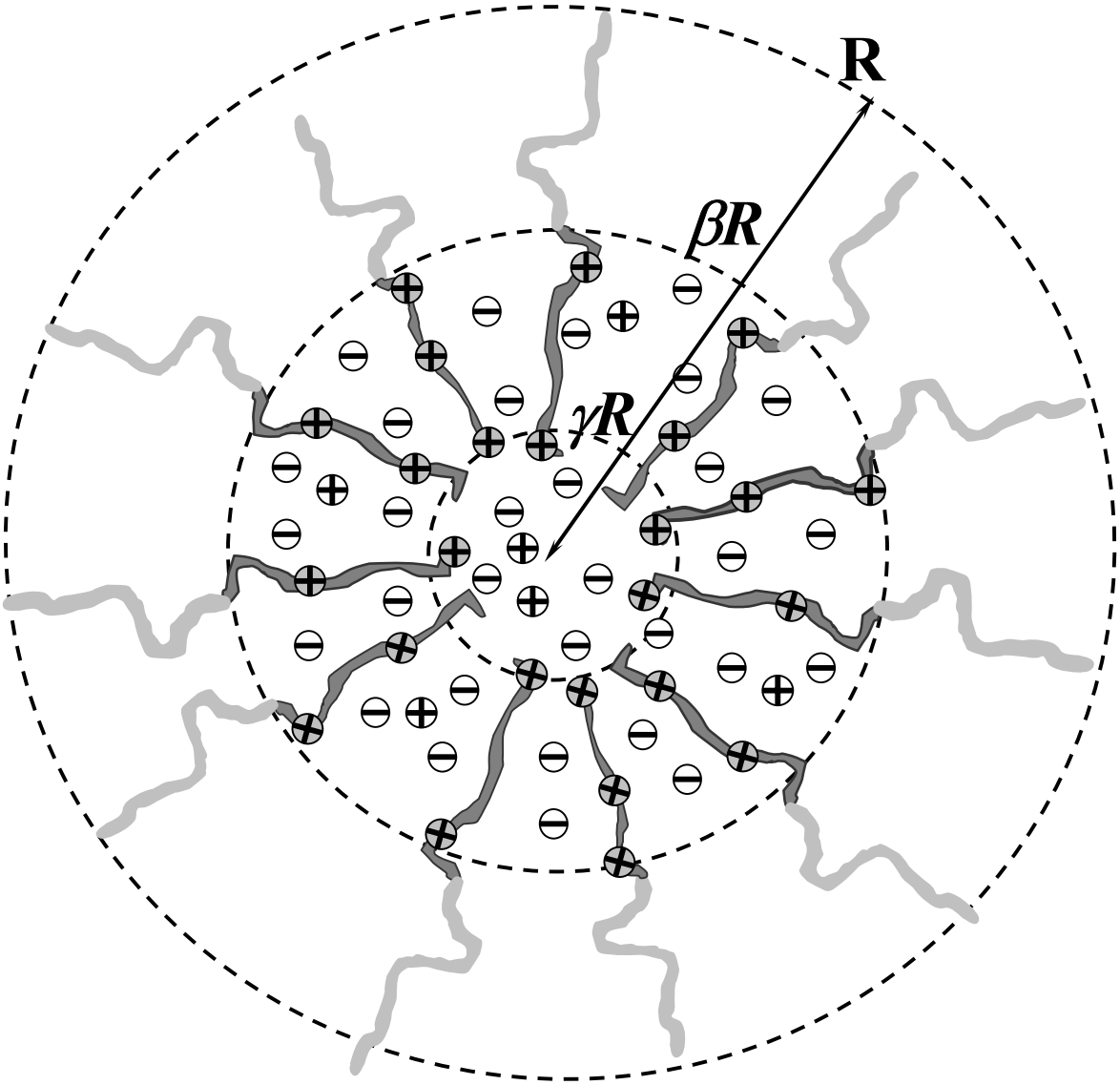

Figure 1 Microdomain of a swollen diblock-copolymer hydrogel with an outer hydrophobic part on the periphery, an inner hydrophilic part containing solvent, mobile monovalent salt ions and fixed charges on the polymer chains. A solvent pool with mobile ions is in the microdomain center

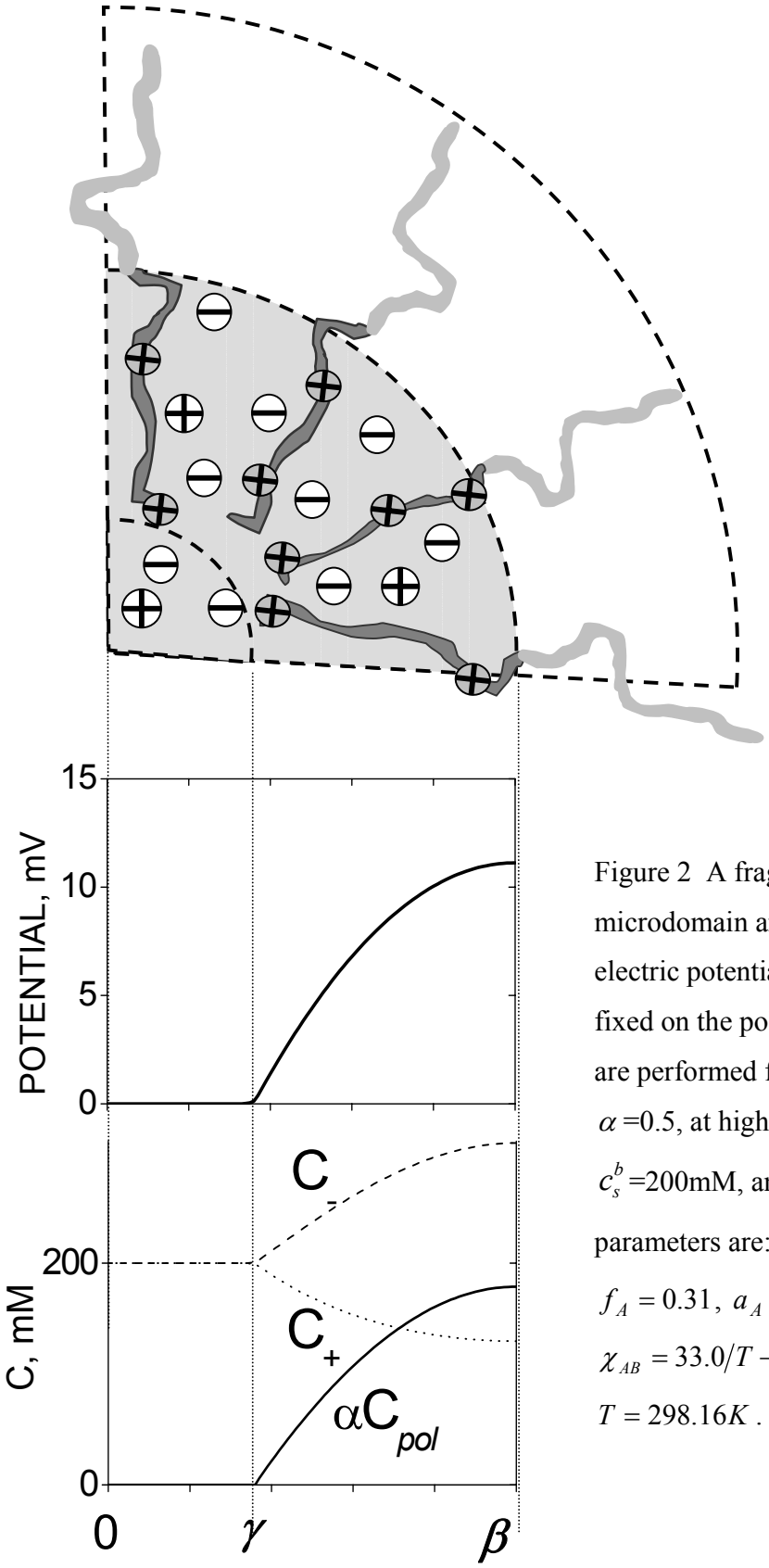

Figure 2 A fragment of the gel microdomain and calculated profiles of electric potential, mobile ions and charge fixed on the polymer chains. Calculations are performed for a strongly charged gel, α =0.5, at high salt concentration, c_s^b =200mM, and φ_s =0.85. Model parameters are: $N = N_A + N_B = 1000$, $f_A = 0.31$, $a_A = a_B = a = 0.68\,\text{nm}$, $\chi_{AB} = 33.0/T - 0.0228$, $\chi_{AS} = 0$, $T = 298.16K$.

Figure 3 Predicted distribution of electric potential, mobile ions and fixed charge across the microdomain shown in Figure 2. Low salt concentration: c_s^b=1.7mM. α=0.05, φ_s=0.80, other parameters as in Figure 2.

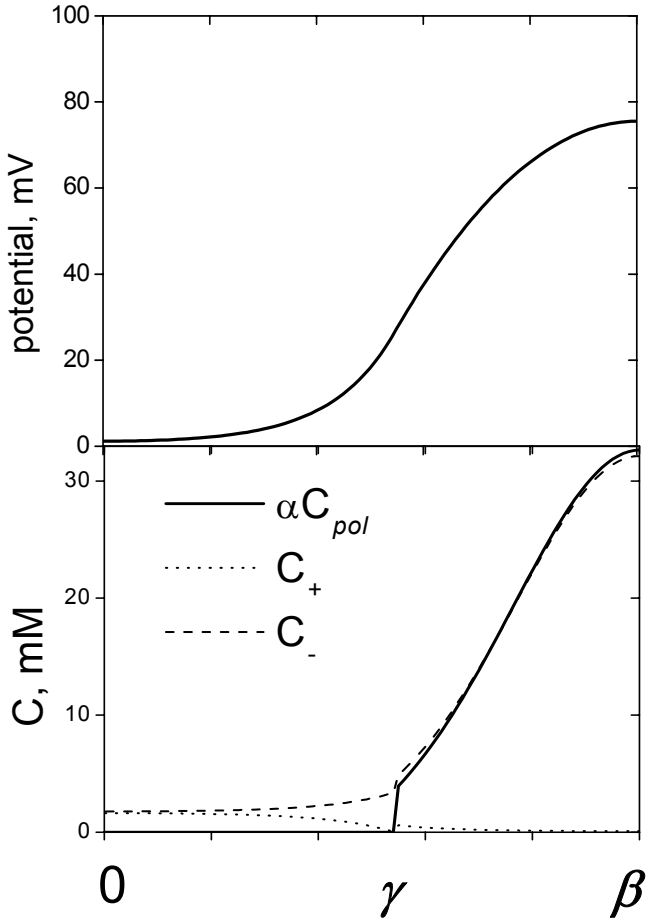

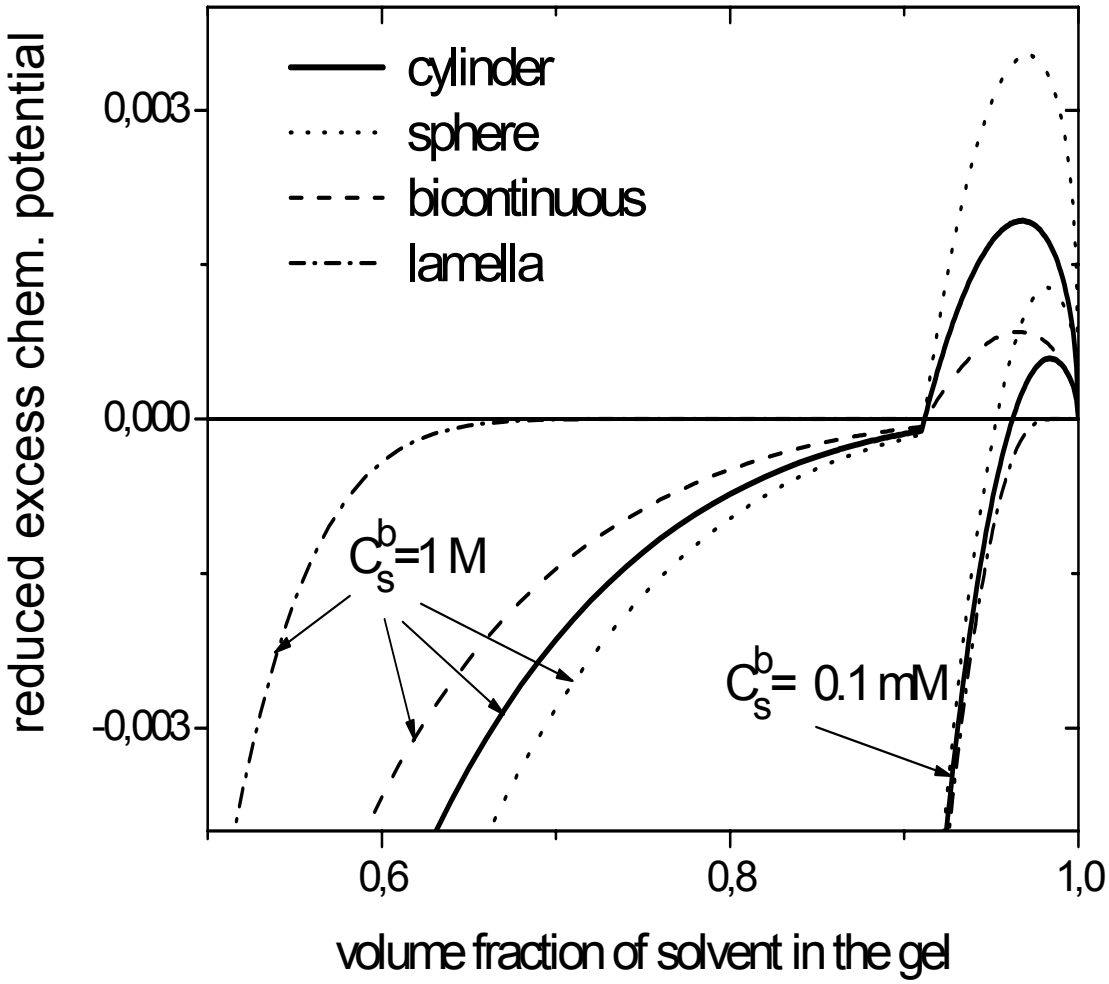

Figure 4 Effect of salt concentration in external solution on the excess chemical potential (in units of kT) of solvent in the gel over that in the external solution for ionic gels of different morphologies. Equilibrium swelling of the gel corresponds to zero of the excess chemical potential. Fraction at preparation of the gel is φ_s^*=0.91, $N = N_A + N_B = 460$; α=0.01; other model parameters as in Figure 2.

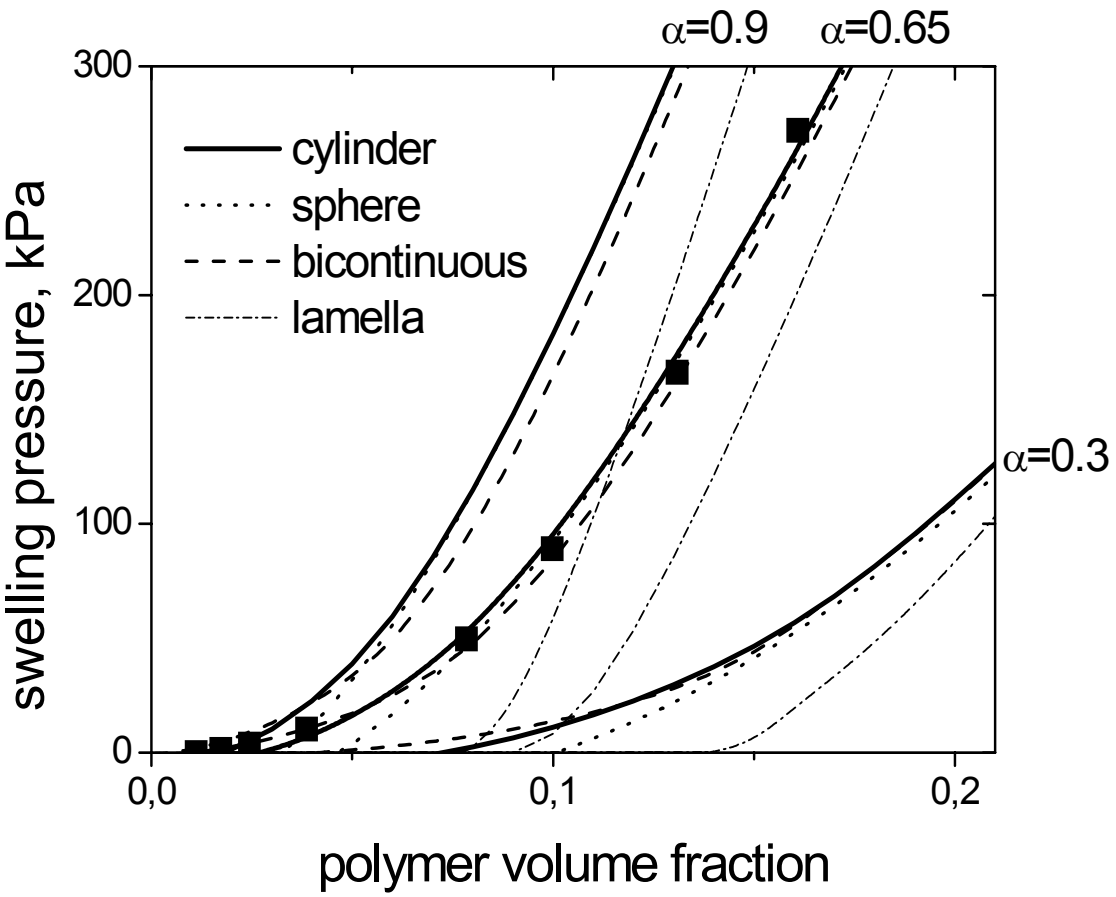

Figure 5 Effect of the assumed ionic charge and microdomain shape on the calculated swelling pressure (curves) and experimental data (points) for a sodium polyacrylate hydrogel [12] at C_{NaCl}=40mM. Polymer fraction at preparation of the gel is ca. 0.3 vol.%. $N = N_A + N_B = 460$; other model parameters as in Figure 2.

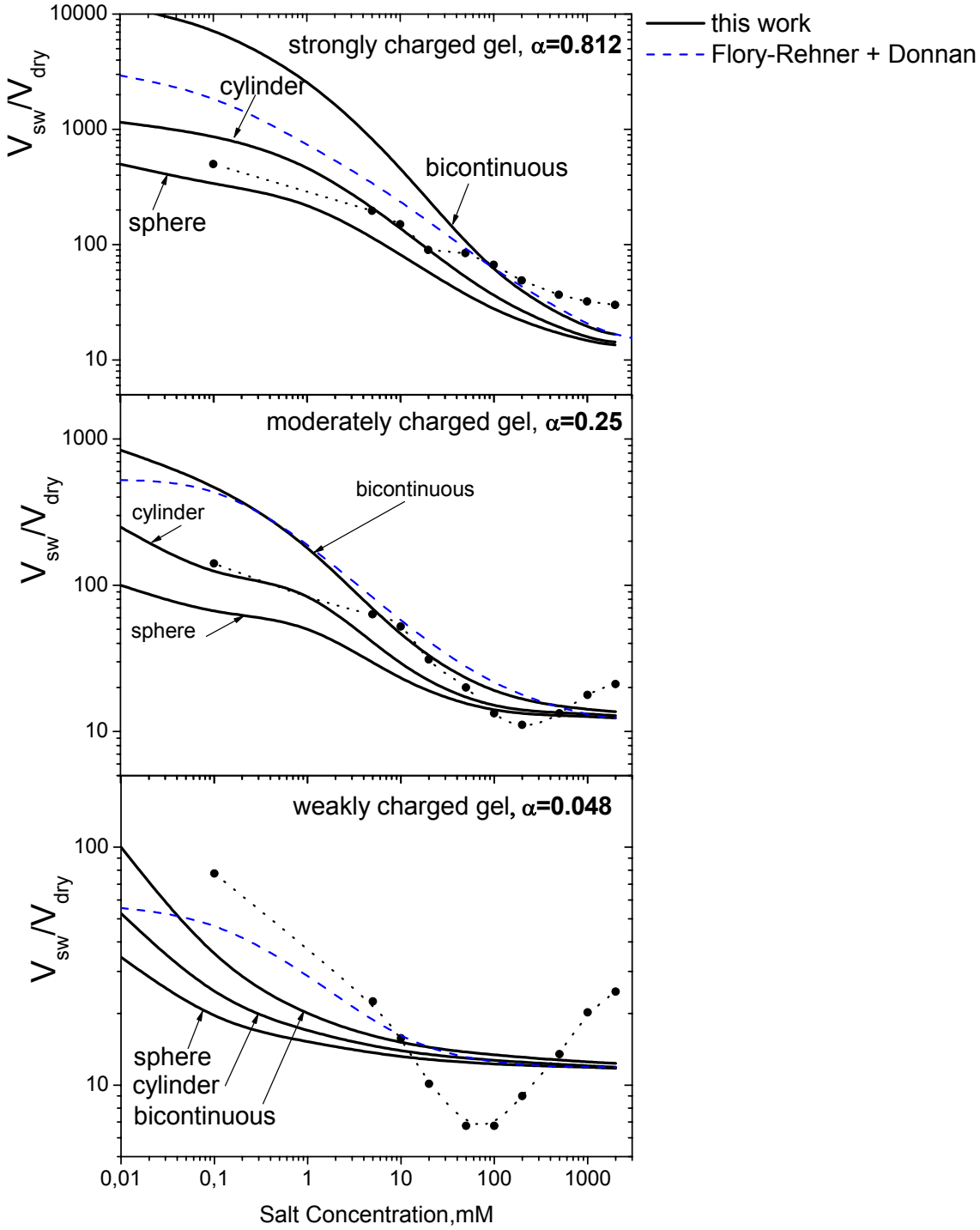

Figure 6 Calculated equilibrium swelling (ratio of swollen-to-dry gel volumes) versus salinity of the bulk solution for gels of different ionic charge and morphology. Model parameters as in Figure 2. Results of the classical Flory-Rehner+Donnan theory, Equation (41), are given for

N_c =101. Points show experimental data [9] for a microphase-separated polyacryl-based hydrogels prepared at ca. 470-460mM polymer.

References

1 D. Sweeney, *Silicone hydrogels : the rebirth of continuous wear contact lenses* (Butterworth Heinemann, Oxford ; Boston, 2000).

2 S. Kimura, T. Kidchob, and Y. Imanishi, Polymers for Advanced Technologies **12**, 85 (2001).

3 A. Katchalsky and I. Michaeli, Journal of Polymer Science **15**, 69 (1955).

4 A. Katchalsky and M. Zwick, Journal of Polymer Science **16**, 221 (1955).

5 J. Hasa, M. Ilavsky, and K. Dusek, Journal of Polymer Science: Plymer Physics Edition **13**, 253 (1975).

6 H. H. Hooper, J. P. Baker, H. W. Blanch, J.M. Prausnitz, Macromolecules **23**, 1096 (1990).

7 E. Vasheghani-Farahani, J. H. Vera, D. G. Cooper, M. E. Weber, Industrial and Engineering Chemical Research **29**, 554 (1990).

8 S. A. Dubrovskii and G. A. Rakova, Macromolecules **30**, 7478 (1997).

9 G. Nisato, J. P. Munch, and S. J. Candau, Langmuir **15**, 4236 (1999).

10 A. E. English, T. Tanaka, and E. R. Edelman, Macromolecules **31**, 1989 (1998).

11 F. Horkay, I. Tasaki, and P. J. Basser, Biomacromolecules **2**, 195 (2001).

12 F. Horkay, P. J. Basser, A.-M. Hecht, E. Geissler, Macromolecules **33**, 8329 (2000).

13 F. Horkay, I. Tasaki, and P. J. Basser, Biomacromolecules **1**, 84 (2000).

14 A. Fernandez-Nieves, A. Fernandez-Barbero, and F. J. de las Nieves, Journal of Chemical Physics **115**, 7644 (2001).

15 M. Moffit, K. Khougaz, and A. Eisenberg, Acc. Chem. Res. **29**, 95 (1996).

16 L.-F. Zhang, K. Yu, and A. Eisenberg, Science **119**, 3168 (1996).

17 A. Eisenberg and J.-S. Kim, *Introduction to ionomers* (Wiley, New York, 1998).

18 K. Yoshikawa, A. Desjardins, J. Dealy, A.Eisenberg, Macromolecules **29**, 1235 (1996).

19 Z. Fang, S. Wang, S.-Q. Wang, J.P.Kennedy, Journal of Applied Polymer Science **88**, 1516 (2003).

20 Y. Ma, G. Wu, and W. Yang, Journal of Polymer Science: Polymer Chemistry **41**, 2755 (2003).

21 M. Shibayama, Y. Fujikawa, and S. Nomura, Macromolecules **29**, 6535 (1996).

22 R. F. Storey and D. W. Baugh, Polymer **42**, 2321 (2001).

23 P. Kurian and J. P. Kennedy, Journal of Polymer Science: Part A: Polymer Chemistry **40**, 1209 (2002).

24 P. J. Flory, *Principles of polymer chemistry* (Cornell University Press, Ithaca,, 1953).

25 T. M. Birshtein and V. M. Amoskov, Polymer Science, Ser. C **42**, 172 (2000).

26 S. Misra and S. Varanasi, Journal of Chemical Physics **95**, 2183 (1991).

27 Y. V. Lyatskaya, F. A. M. Leermakers, G. J. Fleer, E.B.Zhulina, T.M.Birshtein, Macromolecules **28**, 3562 (1995).

28 Y. Lyatskaya and A. C. Balazs, Macromolecules **29**, 5469 (1996).

29 E. B. Zhulina, J. K. Wolterink, and O. V. Borisov, Macromolecules **33**, 4945 (2000).

30 E. B. Zhulina, O. V. Borisov, J. van Male, F.A.M.Leemakers, Langmuir **17**, 1277 (2001).

31 E. B. Zhulina and O. V. Borisov, Journal of Chemical Physics **107**, 5952 (1997).

32 E. B. Zhulina, T. M. Birshtein, and O. V. Borisov, Macromolecules **28**, 1491 (1995).

33 M. Rubinstein, R. H. Colby, A. V. Dobrynin, J.-F. Joanny, Macromolecules **29**, 398 (1996).

34 O. V. Borisov and E. B. Zhulina, Macromolecules **36**, 10029 (2003).

35 V. V. Vasilevskaya, A. A. Aerov, and A. R. Khokhlov, Journal of Chemical Physics **120**, 9321 (2004).

36 R. E. Limberger, I. I. Potemkin, and A. R. Khokhlov, Journal of Chemical Physics **119**, 12023 (2004).

37 A. I. Victorov, C. J. Radke, and J. M. Prausnitz, Molecular Physics **100**, 2277 (2002).

38 A. I. Victorov, C. J. Radke, and J. M. Prausnitz, Molecular Physics **103**, 1431 (2005).

39 R. M. Fuoss, A. Katchalsky, and S. Lifson, Proceedings of the National Academy of Sciences of the United States of America **37**, 579 (1951).

40 A. N. Semenov, Macromolecules **26**, 6617 (1993).

41 I. W. Hamley, *The physics of block copolymers* (Oxford University Press, Oxford ; New York, 1998).

42 E. B. Zhulina and O. V. Borisov, Macromolecules **31**, 7413 (1998).

43 S. T. Milner, Macromolecules **27**, 2333 (1994).

44 P. D. Olmsted and S. T. Milner, Macromolecules **31**, 4011 (1998).

45 M. W. Matsen and F. S. Bates, Macromolecules **29**, 7641 (1996).

46 G. Nisato, F. Schosseler, and S. J. Candau, Polymer Gels and Networks **4**, 481 (1996).

47 T. L. Hill, *An introduction to statistical thermodynamics* (Addison-Wesley Pub. Co., Reading, Mass., 1960).

48 S. A. Safran, *Statistical thermodynamics of surfaces, interfaces, and membranes* (Addison-Wesley Pub., Reading, Mass., 1994).

49 R. J. Hunter, *Foundations of Colloid Science* (Oxford University Press Inc., N.Y., 1995).

50 J. N. Israelachvili, *Intermolecular and Surface Forces* (Academic Press Ltd., Second Edition, San Diego, CA, 1995).

51 R. J. F. Leote de Carvalho, E. Trizac, and J.-P. Hansen, Physical Rewiev E **61**, 1634 (2000).

52 E. K. Zholkovskij, S. S. Dukhin, N. A. Mishchuk, J. H. Masliyah, J. Czarnecki, Colloids and Surfaces A: Physicochemical and Engineering Aspects **192**, 235 (2001).

53 E. Trizac and J.-P. Hansen, Physical Review E **56**, 3137 (1997).

54 G. B. Arfken and H.-J. Weber, *Mathematical methods for physicists* (Academic Press, 2001).